UNIVERSIDADE DE SÃO PAULO

INSTITUTO DE FÍSICA
CAIXA POSTAL 20516
01498 - SÃO PAULO - SP
BRASIL

PUBLICAÇÕES

IFUSP/P-933

ELECTRIC FIELD GRADIENT IN Zr_3Fe, Zr_2Fe AND Zr_2Cu

Helena M. Petrilli and Sonia Frota-Pessôa
Instituto de Física, Universidade de São Paulo

Agosto/1991

"Electric Field Gradient in Zr_3Fe, Zr_2Fe and Zr_2Cu"

Helena M. Petrilli and Sonia Frota-Pessôa, Instituto de Física da Universidade de São Paulo, Caixa Postal 20516, 01498 São Paulo-SP, Brazil.

In this paper we obtain the electric field gradient at the nucleus (EFG) for each non-equivalent site of the crystalline compounds Zr_3Fe, Zr_2Fe and Zr_2Cu. The results agree well , in magnitude and sign, with available experimental results in the literature. The distances and exact coordinates for the Fe site in the orthorhombic Zr_3Fe are uncertain. We have performed calculations for several positions of the Fe in o-Zr_3Fe and found a very stable value of the EFG but the asymmetry parameter η is extremely dependent on the position of the Fe atom. In field Mössbauer measurements for this alloy indicates that the value of η should be close to zero at this site. We use these measurements and our results to estimate the position of the Fe atom in the orthorhombic structure.

Calculations were performed using both the standard first-principles linear muffin-tin orbital method (LMTO) and the recently developed real-space scheme which allows us to obtain the EFG in metallic alloys. This scheme, based on the recursion method and on the LMTO formalism in the atomic sphere approximation (ASA), does not involve any adjustable parameters, does not require symmetry and can easily be applied to non-periodic systems.

I. Introduction

The electric field gradient at the nucleus (EFG) in solids can be measured using several technics.[1,2] A large number of experiments have been performed to study the EFG in transition metal alloys, including amorphous systems, in order to obtain clues about the local environment and chemical ordering in these materials. But the progress regarding the theoretical understanding of this property has been slow.[3] It is usual to divide the contributions to the EFG in an electronic part due to the electrons close to the nucleus and a lattice contribution due to the rest of the system. The electronic contribution is dominant and very hard to obtain.[3] It mainly depends on very small differences (of order of 0.01 electrons) between the occupations of orbitals with different symmetry around the nucleus. This requires a very good description of the electronic structure which, depending on the system being considered, is not a simple task. Therefore for a long time the EFG measurements have been interpreted using empirical models that take the electronic contribution to be proportional to that of the lattice. The lattice contribution is then obtained using simple point charge models[4] and traditionally include a term enhanced by the Sternheimer factor, to account for an eventual polarization of core electrons. Some evaluations of the electronic contribution directly from band structure calculations have been performed with encouraging results.[5] For transition metals reliable first-principles calculations of the EFG, even in simple crystalline solids, have only recently become available. In 1988

Blaha et al[6] used the full potential (FP) linear augmented plane wave (LAPW) method to obtain the EFG of a series of metals which form in the hcp structure. The charge density used to calculate the EFG is obtained in a self consistent manner using the local density approximation and no empirical factors were used. The core polarization in these metals was found to be extremely small and could in fact be neglected.

Once a reliable result is available to be used as control, other methods to obtain the EFG in metals could be tested. We have recently developed a formalism implemented in real-space which allows us to obtain the dominant electronic contribution to the EFG for systems well represented by a tight-binding (TB) Hamiltonian.[7] This method uses the LMTO-ASA formalism in the TB representation[8] to build the Hamiltonian and was applied with success[9] to obtain the EFG in the same hcp metals used in the FP-LAPW calculations. The electronic contributions due to p and d electrons in all cases agree in sign and magnitude with those obtained by Blaha et al in ref.(6). The results for the total EFG have the correct sign and the magnitude agrees within a factor of two with experiment and with the FP-LAPW results. This agreement is remarkable considering the lack of adjustable parameters and the subtlety of the effect. Reciprocal space results for the electronic contribution to the EFG using the standard LMTO-ASA formalism were also obtained. The agreement with the FP-LAPW results was similar to that of the real-space calculations indicating that the main limitations are the approximations used in the LMTO-ASA approach and are not inherent

to the real-space scheme. In both LMTO-ASA calculations the lattice contribution, which is due to charges outside the Wigner-Seitz (WS) sphere around the atom, was neglected. According to the FP-LAPW results, the lattice contribution is typically one order of magnitude smaller than the electronic contribution for these systems.

The LMTO-ASA is a very fast tool[10] and the real space approach does not require periodicity. Actually it was recently used to obtain the distribution of EFG in a cluster of amorphous Zr.[11] Therefore we feel encouraged to continue research in this field, applying the method to obtain the EFG in binary alloys. In this paper we apply the LMTO-ASA real-space scheme to calculate the electronic contribution to the EFG at every non-equivalent site in three crystalline Zr alloys: Zr_3Fe, Zr_2Fe and Zr_2Cu. We have also performed k-space standard LMTO-ASA calculations for these materials. The behavior of the EFG at the Fe site in the Zr-Fe alloys is an interesting example of the influence of local environment over this property. The Zr site in Zr_2Cu has a very small measured EFG, but the Zr sites in amorphous Zr-Cu alloys seem to have a much larger EFG.[12,13] In field Mössbauer measurements[14] of the EFG at the Fe site, show a negative value for tetragonal Zr_2Fe, but a positive value for orthorhombic Zr_3Fe. These results have been used in attempts to understand the structure of amorphous Zr-Fe alloys.[15] In a recent communication[16] we show that real-space calculations of the EFG at the Fe site also give opposite signs for this quantity in the two Zr-Fe compounds. In the present paper we investigate the behavior of the EFG in

these interesting crystalline Zr based compounds, using the results of electronic structure calculations. We obtain the EFG at every site for these alloys. For several of the sites the value for the EFG has not been measured. We hope that our results will help in the interpretation of the available data and encourage further measurements of the EFG in these materials.

In Section II we give a brief description of the LMTO-ASA recursion approach used in the real-space electronic structure calculations. In section III we show how the EFG tensor can be obtained from these calculations. Results and discussions are presented in section IV. Finally in section V we have the conclusions.

II. The LMTO-ASA-TB approach

Real-space methods such as the recursion method[17] are very efficient when the system is well described by a TB Hamiltonian. The LMTO-ASA formalism in the tight-binding representation[8] provides the theoretical basis for the construction of reliable TB Hamiltonians for close packed transition metal systems. Within the LMTO-ASA formalism, a good parametrized TB Hamiltonian can be obtained without the need of fitting procedures to experimental results or more exact calculations and there are no adjustable parameters. As an extra benefit we can evaluate the wave function and properties that depend on it. A detailed description of the parametrized LMTO-ASA recursion real-space scheme is given elsewhere.[18] The theory behind the parametrization LMTO-ASA-TB used in the present calculations is also explained there. In this

section only a brief description of the main results will be given to guide the reader and establish the notation.

The LMTO is a linear method and its solutions are valid around a given energy E_ν, normally chosen at the center of gravity of the occupied part of each (s, p or d) band. When solving the problem in real-space, we work in the first order approximation, neglecting terms of order of $(E-E_\nu)^2$ and higher. One of the characteristics of the LMTO-ASA formalism is that we can generate new basis sets, with desired properties, through a controlled mixing of the functions of the standard LMTO base.[8] There are three very important LMTO-ASA basis: the standard, the nearly orthogonal and the tight-binding (also known as the most localized) basis set.[19] The standard representation can be seen as the one with no mixing, and the mixing parameter is zero. In the nearly orthogonal representation the mixing Q_ℓ is chosen to make the overlap matrix close to unity. In the tight-binding or most localized representation the mixing $\overline{Q}_\ell$ is chosen in order to make the interactions between neighboring sites in the Hamiltonian as short ranged as possible. As we will see the mixing parameters $\overline{Q}_\ell$ are approximately independent of the material. Here as in the rest of the paper unbarred quantities designate orthogonal parameters and barred quantities most localized ones. It can be shown that up to first order in $(E-E_\nu)$, the orthogonal and the TB representations are equivalent.[19]

In the LMTO-ASA, space is filled with WS spheres centered at all atomic sites. The potential is assumed to have spherical symmetry around each sphere. Within the ASA approximation the problem of solving for the electronic structure is divided in

two parts. The first part involves finding the solution of the radial Schroedinger equation inside each WS sphere, with given boundary conditions, to obtain the values of the potential parameters C_ℓ, Δ_ℓ and Q_ℓ which are used to construct the Hamiltonian. The solution $\varphi_\nu(r)$ of the radial part of the Schroedinger equation within each sphere at energy E_ν and its energy derivative $\dot{\varphi}_\nu(r)$ at E_ν are important quantities in the formalism. The values of $\varphi_\nu(r)$ and $\dot{\varphi}_\nu(r)$ are taken to be zero outside their own sphere. In the orthogonal representation the wave function is expressed as a linear combination of these functions at each site. The second part of the problem is to find the structure constant matrix, which depends only on the structure. The structure constant matrix S^0 of the standard representation, also known as canonical structure constant, is given by the coefficients of the expansion of the tail of a muffin-tin orbital centered at $\vec{R}$, around any other site $\vec{R}'$. It is given by the well-known expansion:[20]

$$\left[\frac{r_R}{a}\right]^{-\ell-1} Y_L(\hat{r}_R) = -\sum_{L'} \left[\frac{r_{R'}}{a}\right]^{\ell'} \frac{Y_{L'}(\hat{r}_{R'})}{2(2\ell'+1)} S^0_{R'L',RL} \qquad (1)$$

where $L=(\ell,m)$ is a collective angular momentum index and the notation $r_R = |\vec{r}-\vec{R}|$ was used. The coefficients $S^0_{R'L',RL}$ are well determined and given in the literature.[19] These coefficients do not depend on the material or type of atoms being considered, but only on the position of the sites for the given structure.

When solving the problem in real-space using the first order approximation it is convenient to work in the orthogonal

representation, expressing the orthogonal Hamiltonian in terms of TB parameters. This is possible because the sets for the several representations are related through mixing. When this is done we have a simple eigenvalue problem to solve:

$$(H - E)u = 0 \qquad (2)$$

where H is given by:[19]

$$H = \bar{C} + \bar{\Delta}^{1/2} \bar{S} \bar{\Delta}^{1/2} \qquad (3)$$

Once the eigenvalue problem is solved, the wave function is given by:

$$\chi_E(\vec{r}) = \sum_{RL} \left\{\varphi_{\nu\ell}(r_R) + (E - E_{\nu\ell R})\, \dot{\varphi}_{\nu\ell}(r_R)\right\} Y_L(\hat{r}_R)\, u_{R,L}(E) \qquad (4)$$

The structure constant matrix $\bar{S}$ for a system defined by the mixing $\bar{Q}_\ell$ can be obtained from the canonical structure matrix S^0 using the expression:[19]

$$\bar{S} = S^0(I - \bar{Q}S^0)^{-1} \qquad (5)$$

Here I is the unit matrix and $\bar{Q}$ is a diagonal matrix with elements $\bar{Q}_\ell$. The mixing of the TB representation was found by trial and error[8] by varying $\bar{Q}$ in expression (5) in order to obtain the most localized structure-constant matrix $\bar{S}$. The values of the mixing were found to be approximately independent of the structure and when s, p and d orbitals are considered, they are given by the constants $\bar{Q}_s = 0.3485$, $\bar{Q}_p = 0.0530$ and $\bar{Q}_d = 0.01071$.[8,19] To find $\bar{S}$ it is sufficient to obtain the 9x9 matrices connecting one site to its neighbors as well as the onsite term (a 9x9 matrix connecting the site to itself). It is not necessary to invert a matrix representing all atoms in the cluster. It is normally sufficient to take the site and its close neighbors. Here, to obtain $\bar{S}$ around

each site in the primitive cell, we invert the matrix for a cluster containing approximately 20 sites.[18] We note that $\bar{S}$ decays exponentially with the distance to the neighboring sites. Only close neighbors are connected through hopping, giving rise to a very tightly bound Hamiltonian for s, p and d electrons.

To build the Hamiltonian we also need the potential parameters $\bar{C}_\ell$ and $\bar{\Delta}_\ell$. Again because the several representations are related through mixing, these TB parameters can be obtained from the orthogonal potential parameters C_ℓ, Δ_ℓ and Q_ℓ. For a given energy E_ν, the relation between these parameters is given by:[19]

$$\frac{\bar{C}_\ell - E_{\nu\ell}}{\bar{C}_\ell - E_{\nu\ell}} = \frac{\bar{\Delta}\ell^{1/2}}{\Delta\ell^{1/2}} = 1 - (Q_\ell - \bar{Q}_\ell)\ \frac{C_\ell - E_{\nu\ell}}{\Delta_\ell} \qquad (6)$$

In the parametrized LMTO-ASA scheme used here, the TB structure constant $\bar{S}$ is exact, but the potential parameters $\bar{C}_\ell$ and $\bar{\Delta}_\ell$ for each atomic species, are obtained using the potential parameters C_ℓ, Δ_ℓ and Q_ℓ of the corresponding pure metallic system, in the orthogonal representation. The orthogonal parameters C_ℓ, Δ_ℓ and Q_ℓ for all the pure transition metals are tabulated in the literature.[19] The TB parameters $\bar{C}_\ell$ and $\bar{\Delta}_\ell$ for the initial calculation are obtained using the above equation. The relative position of the bands in the compound is found by changing the relative position of the center of the bands of the different atomic species in the compound, in order to have approximate charge neutrality.[18] We found that the EFG is very sensitive to small variations of the structure constant, but not very sensitive to small differences in the potential parameters. Therefore the very practical two center form suggested by Andersen et al. to obtain

the TB structure constant should not be used in the context of EFG calculations, but tabulated values of potential parameters are usually good enough.[7,9]

III- The Electric Field Gradient Tensor

In a previous paper[7] we have developed a scheme based on the recursion method to obtain the EFG for systems which are well described by a TB Hamiltonian. The scheme is implemented in real space and can be applied to both, ordered and disordered, close packed metallic systems. If we have a local energy independent basis set $\{\phi_{m,R}\}$ the wave function $|\psi_E\rangle$ can be expanded as:

$$|\psi_E\rangle = \sum_R \sum_{m=1}^{9} u^{(E)}_{m,R}\ |\phi_{m,R}\rangle \qquad (7)$$

Here R is a vector indicating the position of the site and m gives the orbital. The functions $|\phi_{m,R}\rangle$ are chosen to be real and the nine orbitals in each site are designated by s, x, y, z, xy, yz, zx, x^2-y^2, $3z^2-r^2$, characterizing one s orbital, three p orbitals and five d orbitals. The EFG at the nucleus is a local quantity and can be written in terms of the electronic wave function $|\psi_E\rangle$ and the electrostatic potential V(r) around the given nucleus, as a 3x3 tensor with components V_{ij} as:

$$V_{ij} = 2 \int^{E_F} \langle \psi_E \mid \frac{\partial^2 V(r)}{\partial x_i \partial x_j} \mid \psi_E \rangle\ dE \qquad (8)$$

where x_i = x, y or z and E_f is the Fermi energy.

The tensor is traceless and symmetric and has in general only five independent components. It can always be diagonalized to find the local principal axis at the given site. When this is done, the eigenvectors are associated with the three non zero components of the diagonal tensor, but because it is traceless only two of the components are independent. The measured EFG is associated with the component of the diagonal tensor with the largest absolute value. The direction of the EFG is indicated by the eigenvector associated with this component.

If we substitute the wave function $|\psi_E>$ in Eq. (8) by its expression of Eq. (7) and neglect contributions associated with electrons in sites R' different from R, we can obtain the six components V_{ij} of the local EFG tensor at R.[7] They will be expressed in terms of two quantities, the generalized occupation $n_{m,m'}$ and the radial integrals $I_{mm'}$. The $n_{m,m'}$ are given in terms of the partial local density of states (LDOS) and related quantities, and can be obtained by solving the eigenvalue problem for a TB Hamiltonian expressed in the local basis set $\{\phi_{m,R}\}$.[7] The $I_{mm'}$ are calculated using the radial parts of the corresponding basis functions $|\phi_{m,R}>$ at the site R.[7]

The real-space LMTO-ASA-TB formalism described in the last section gives rise to a local basis. The wave function given in Eq. (4) of last section is very similar to that of Eq. (7), but it has a energy dependent radial part. The generalization of the treatment of the components V_{ij} to include the energy dependence

of the radial part is trivial, but new terms appear giving rise to long and cumbersome expressions. Luckily these extra terms are two orders of magnitude smaller than those originating from the energy independent part and can be neglected. Therefore V_{ij} can be obtained from the simpler expressions for an energy independent basis using for $\{\phi_{m,R}\}$ the energy independent part of the LMTO-ASA set, and the radial part $\varphi_{\nu,m}(r)$ defined inside the WS sphere at site R. The expressions for V_{ij} in terms of $n_{m,m'}$ and $I_{mm'}$ are given elsewhere[7]. Within the LMTO-ASA notation of the previous section we have for the generalized occupation:

$$n_{m,m'} = \int^{E_f} u_{m,R}(E)\, u_{m',R}(E)\, dE \qquad (9)$$

When the two indices are the same (m=m') the above expression is equal to the occupation per spin of the orbital m. In this case we suppress one of the indices and define the occupation per spin of the orbital as n_m. The radial integrals $I_{mm'}$ can be written in terms of the radial parts of the solutions of the Schroedinger equation inside the WS sphere around the nucleus, at energy E_ν, as:

$$I_{m\,m'} = \int_0^\infty \frac{\varphi_{\nu,m}(r)\,\varphi_{\nu,m'}(r)}{r}\, dr \qquad (10)$$

Due to selection rules obeyed by the Clebsch-Gordan coefficients only I_{pp}, I_{dd} and I_{sd} are present in the expressions for the components of the EFG tensor. The terms involving I_{sd} are extremely small and are usually neglected. To obtain I_{pp} and I_{dd} within the real space parametrized LMTO-ASA-TB scheme, we use the

self-consistent p and d radial solutions, inside a WS sphere of the pure metal. These values are tabulated for some hcp metals[8]. Because these integrals are determined mainly by the behavior of $\varphi_{\nu,\epsilon}(r)$ close to the nucleus, their values are quite transferable when considering the same type of atom in alloys.

As we will see, the magnitudes of the p and d contributions to the EFG are strongly dependent on the value of the radial integrals I_{pp} and I_{dd}, but the sign of the contribution is completely determined by the angular asymmetry, a combination of values of the generalized occupations $n_{m,m'}$, for the alloy. As an example we consider a system with axial symmetry around the z-axis. This is the case of hcp metals, when z is taken along the c-axis of the structure. The EFG tensor will be diagonal and traceless and the magnitude of V_{zz} will be two times that of the V_{xx} and V_{yy} components. In this case the p contribution to the EFG is proportional to I_{pp} and to the angular asymmetry ΔN_p. A similar expression gives the d contribution in terms of ΔN_d. The values of ΔN_p and ΔN_d, in terms of the occupation of the orbital m per spin n_m, are given in the literature[6,7] as:

$$\Delta N_p = n_x + n_y - 2n_z$$
$$\Delta N_d = 2(n_{xy} + n_{x^2-y^2} - n_{3z^2-r^2}) - n_{xz} - n_{yz} \qquad (11)$$

The values of the angular asymmetries ΔN_p and ΔN_d are extremely small, usually of the order of 0.01 electrons[7,9]. Errors of this order in the differences of occupations can introduce large variations on the magnitude and even change the sign of the EFG[9].

This gives an idea of the accuracy needed, and shows the complexity of the EFG calculations.

In the present paper we also use reciprocal space calculations to obtain the EFG. In this case we perform a regular k-space LMTO-ASA band structure calculation to obtain the self-consistent electronic charge density. By solving the Poisson's equation for the total charge density, the electrostatic potential is obtained. The leading terms of the l=2 components of this potential near the nucleus determine the EFG tensor. In general, a 3X3 matrix must be diagonalized to obtain the EFG. The procedure is similar to the one used by Blaha et al[6]. in their LAPW calculations, but here we only consider the influence of the charge in the WS sphere around the given nucleus[9].

V. Results and Discussion

We have applied the real-space scheme described in the previous sections to calculate the EFG at each non-equivalent site in three crystalline alloys: Zr_2Fe, Zr_3Fe and Zr_2Cu. To check our results we have also used standard k-space LMTO-ASA calculations to obtain the EFG in these alloys. In this first procedure the recursion[17] method is used to solve the eigenvalue problem in real-space and obtain the LDOS for each inequivalent atom. The recursion method is also used to obtain occupations n_m and the off-diagonal terms $n_{m,m'}$, which appear in the expressions for the components of the EFG tensor[7]. In the present calculations we use very large clusters (1000-2000 atoms) and take a cutoff parameter

LL = 20 in the recursion chain. A Beer and Pettifor[21] terminator is then used to obtain the LDOS and related quantities. To build the Hamiltonian in real-space, we have used the parametrized LMTO-ASA-TB approach described above. The TB structure constant matrix $\bar{S}$ was obtained by direct inversion. The potential parameters $\bar{C}_\ell$, and $\bar{\Delta}_\ell$ were calculated using the tabulated values[19] of the potential parameters C_ℓ, Δ_ℓ and Q_ℓ for pure metallic Zr, Fe and Cu, and the relative position of the bands in the compounds were then fixed by imposing approximate charge neutrality[18]. No adjustable parameters were used. In all cases the calculated values of the EFG are very stable and do not depend on the small charge transfers which we may have eventually ignored. This can be easily understood if we remember that the EFG originates from small differences in the occupations of orbitals of different symmetry around the nucleus. These differences develop along the whole occupied bands. The fact that the partial LDOS have different shapes for the different orbitals, is generally more important to the value of the EFG, than the detailed behavior of the LDOS at the Fermi level. As we have mentioned before, in the present paper we calculate the dominant contribution to the EFG, which arises from the valence electrons within the WS sphere around the nucleus. This is the case for both, real-space and reciprocal-space LMTO-ASA calculations. We find that the p and d terms are the relevant ones in the electronic contribution for the EFG. The s-d terms of the V_{ij} expression[7] give rise to contributions which are generally two orders of magnitude smaller than those of the p and d terms . We have not included here

the lattice contribution, which originates from charges outside the central WS sphere, and is normally ten times smaller than the electronic contribution in these materials[8]. The core contribution seems to be smaller than the lattice contribution by an order of magnitude[6], and was also neglected.

Our aim here is to have a complete description of the behavior of the EFG for all sites in the three Zr compounds. For every site, we have calculated the components of the EFG tensor, using both real and k-space methods. Those 3 x 3 matrices were then diagonalized in order to find the local principal axis and the value of the EFG. Another measurable quantity that can be obtained from the components of the electric field gradient tensor is the asymmetry parameter η. It is defined as the difference between the two smaller components of the tensor in the principal axis, divided by the largest one. This quantity is always defined as positive and is zero when the system has axial symmetry around the site[2]. To have a more complete understanding of the problem we have also splitted the components of the EFG tensor into p and d contributions and have found the local principle axes for each of the two (p and d) terms. In table 1 we show the values obtained for the EFG for Zr_2Fe, Zr_3Fe and Zr_2Cu using the LMTO-ASA formalism in real space and k-space as described above. For comparison we also show the values for the EFG at the Fe sites, obtained from experimental data available in the literature[14]. To obtain the measured value of the EFG for the Fe sites shown in Table 1, we have used 0.2b for the nuclear quadrupole moment of ^{57}Fe. We note that the experimental value for the EFG at the Zr

site in Zr_2Cu which appears in Table 1, was actually obtained using a Hf probe. We could not find in the literature measurements for the EFG at the Cu site in Zr_2Cu, or for the EFG at the Zr sites for the Zr-Fe compounds. From Table 1 we see that the k-space and real-space results agree in sign and magnitude within the expected accuracy. As in the case of the hcp metals[9], the calculated EFG for these three Zr alloys, have the correct sign and agree within a factor of two with the available experimental results.

The results for the EFG are given in Table 1. We now proceed to discuss the detailed behavior of the EFG tensor and related quantities in each of these compounds. In all the calculations we have chosen the x,y and z cartesian axes to be parallel to the a, b and c axes of the given structure. In table 2 we show the values of I_{pp} and I_{dd}, for Zr, Fe and Cu obtained from pure hcp Zr, bcc Fe and fcc Cu, used in the real-space calculations. Exact values for these integrals at the Zr, Fe and Cu sites in Zr_2Fe, Zr_3Fe and Zr_2Cu, were also obtained using our self-consistent k-space LMTO-ASA results. In all cases the values of the integrals obtained for the alloys and for the pure metals are in excellent agreement, differing by less than ten percent. From Table 2 we see that I_{pp} is much larger than I_{dd} in the beginning of the transition-metal series (Zr case), but this difference decreases as the d band is filled and the d orbitals are compressed towards the nucleus. For Cu, at the end of the transition series, the values of I_{pp} and I_{dd} are similar, with the d integral slightly larger.

i) Zr_2Fe has a well known tetragonal structure ($CuAl_2$

(C16) - type structure) with lattice parameters a= 6.385 Å and c = 5.596 Å[22]. There are six atoms on the primitive cell, but all Fe sites have the same LDOS and EFG. All Zr sites also have the same LDOS and the same scalar value of the EFG. The direction of the EFG does not need to be the same for inequivalent Zr atoms in the primitive cell, but once the direction in one of the sites is obtained, the directions in other sites can be easily determined. Therefore only one Fe site and one Zr site have to be considered.

In our real space calculations we have used a cluster of 1785 atoms and obtained the LDOS for a Zr atom and for an Fe atom close to the center of this cluster. We note that in Zr_2Fe, the Fe site has axial symmetry along the z axis and that the EFG tensor at the Fe site is diagonal. The EFG is negative (see Table 1) and along the c axis. We find that in this case both p and d contributions to the EFG are negative and similar in magnitude. The asymmetry parameter η is zero, as expected for sites with axial symmetry. At the Zr site the EFG tensor is not diagonal but the components V_{xz} and V_{yz} are zero. For the given Zr site, the V_{xy} component was found to be positive and much larger (a factor of ten) than the diagonal components. When we diagonalize the tensors for the p, d and total contributions we find in all cases the same set of principal axes. In Table 3 we show the eigenvalues and corresponding eigenvectors (direction cosine of the principal axis with respect to the a,b and c axes of the structure) for the total, the p and the d contributions at the Zr site. For comparison, results obtained using the parametrized real-space LMTO-ASA-TB

approach and those obtained using the standard k-space LMTO-ASA formalism are shown. We note that the two smallest components of the diagonal tensor are very different, indicating a large value for the asymmetry parameter η at the Zr site. We see that the p contribution to the EFG is much larger than the d contribution. This is usually the case at Zr sites (see Table 2), because the integral I_{pp} is much larger than I_{dd} when atoms of this type are considered. From table 3, it is also clear that the c-axis is one of the principal axis of the tensor, but for the other axes we have a rotation of 45 degrees in the x-y plane. Actually the direction of the EFG (largest component in the principal axes) is in the plane perpendicular to the c-axis, and makes 45 degrees with both the a and b-axes. If one looks at the structure of Zr_2Fe described in ref. (22), this direction is along the line that joins the Zr site, the closest Zr neighbor located at a distance d_1 in fig. 8 of ref. (22), and the center of one of the hexagons to which the site belongs.

ii) Zr_3Fe has an orthorhombic Re_3B-type structure with eight atoms on the primitive cell and measured lattice parameters given by a= 3.326 Å, b= 10.988 Å and c= 8.807 Å[23]. This structure is relatively simple, being build up of triangular prisms of 6 Zr atoms surrounding each Fe atom. In this structure the LDOS is the same for all Fe, but there are two types of Zr atoms with different LDOS. This means that we have to consider one Fe site and two Zr sites in our calculations. In Fig. 1 we show a sketch of the orthorhombic structure for Zr_3Fe, where Zr atoms (large spheres) and Fe atoms (small spheres) are shown in a projection over the

plane perpendicular to the a-axis. The empty spheres indicate atoms in the x=0 plane and the dashed ones indicates atoms at a height of a/2 along the a-axis. There are no measurements indicating the exact position of the Fe atom in the cell. In our calculations for the EFG in Zr_3Fe, we have maintained fixed the position of the Zr atoms in the prism and given to the central Fe, small dislocations along the b-axis, as indicated by the arrows in Fig.1. For the Zr atoms we have used the Re_3B atomic parameters given in the literature[24]. For the Fe we have kept the x and z atomic parameters (at x=0.0 and z=0.25)[24], but we have varied the atomic parameter y starting from the value of B in Re_3B (y=0.744)[24], towards smaller values. A smaller value of y will place the Fe site closer to the base of the projected triangle. We note that for the given values of a, b and c in Zr_3Fe, the Fe will be at the center of the prism for an atomic parameter y=0.741. As we have mentioned before there are two types of Zr atoms with different LDOS. These Zr sites have different values for the EFG and will be designated by Zr1 and Zr2. If we look at Fig.1 and consider that the Fe atoms are moving along the height of the projected triangles, Zr1 will be the Zr site at the vertices of the triangle and Zr2 will be associated with the two Zr sites at the base.

In our real-space calculations of the EFG for the several positions of the Fe atom, we have used large clusters, of about 2000 atoms. We find that in orthorhombic Zr_3Fe, the EFG tensor at the Fe site is diagonal and a, b and c are the principal axes of the tensor. Our calculations show that V_{xx} is always the largest

component, indicating a positive EFG directed along the a-axis. The value of the EFG is very stable with respect to small variations of the position of the Fe site in the prism. Therefore the value of the EFG at the Fe site, for Zr_3Fe in Re_3 B-type of structure, is quite well defined, even when the position of the Fe site in the trigonal prism is not exactly determined. Both p and d components of the EFG are positive, and the p contribution is about two times bigger than the d contribution. The agreement between real and k-space is rather good and within the expected accuracy of the calculation. The trace of the EFG tensor is always zero and as a consequence, the sum of V_{zz} and V_{yy} at the Fe site is equal to V_{xx} in magnitude, having the opposite sign. As expected, we find that the sum of the V_{yy} and V_{zz} components is also very stable with respect to small variations of the position of the Fe atom in the structure. But the individual value of each of these two components are more sensitive to these variations giving rise to strong variations of the asymmetry parameter η. In Fig. 2 we show the calculated V_{zz} and V_{yy} components of the EFG tensor at the Fe site in Zr_3Fe as a function of the atomic position parameter y. To treat systematically these small variations we have to minimize the errors and these calculations were performed in k-space. As we can see from the figure, for large values of the position parameter y the value for V_{zz} is larger in magnitude than that of V_{yy}, but as y decreases the magnitude of V_{zz} also decreases, while the magnitude of V_{yy} increases. At the value of y≈ 0.735 the two components are equal. Finally, if we continue to move the Fe site towards the base of the projected triangles, the magnitude of V_{yy}

gets to be larger than the magnitude of V_{zz}. This behavior leads to large variations of the asymmetry parameter η. The value of η is around 0.2 for y= 0.744, goes to zero close to y= 0.735 and increases again for smaller values of y. When the Fe site is placed at the center of the trigonal prism (y ≈ 0.741), the asymmetry parameter η is still quite large, close to 0.1. This is probably due to the effect of a second shell with three Zr atoms around the Fe site, one of them further from the Fe atom than the other two. The reported experimental results gives[14] η = 0 for the Fe site and for this reason the results for the EFG shown in Table 1 are those obtained using y=0.735. It is interesting to note that, in this case, η may give a good criterion for evaluating the atomic position parameter y of the Fe atom. On the other hand, it would be interesting to verify if a small, but finite value of η (around 0.1 as obtained when the Fe is placed at the center of the trigonal prism with y≈0.741) would be compatible with the in field Mössbauer spectra of Zr_3Fe[14].

The Zr1 site of Zr_3Fe has also a diagonal EFG tensor. The EFG is positive and along the c-axis. The components of the EFG tensor at the Zr1 site are almost insensitive to small variations of the Fe atomic position. In k-space as well as in real space, the d and p contributions have the same sign. As it was to be expected in the case of Zr, the d contribution is small, less than 10% of the total EFG. At this site the asymmetry parameter is close to zero.

The Zr2 site of Zr_3Fe has a non-diagonal EFG tensor with V_{xy} and V_{xz}components equal to zero. At the calculated site the V_{yz}

in the case of Zr1, the d contributions to the tensor are much smaller than the p contributions. In the case of Zr2 we find that the principal system of axes is different for p and d contributions. To obtain the EFG, we have to find the largest component of the diagonalized total EFG tensor. We note that in this case the EFG does not, in a natural way, split into p and d contributions. In table 4 we show the eigenvalues and eigenvectors of the total EFG tensor at the Zr2 site. As we can see from the eigenvectors in table 4, in order to find the principal axis, a rotation in the plane perpendicular to the a-axes has to be performed. The EFG at the Zr2 site has negative sign and points into a direction that makes about 30 degrees with the c-axis of the Zr_3Fe structure. It's interesting to note, that although the two Zr2 atoms per unit formula have the same LDOS, before the diagonalization of the total EFG tensor, their V_{zy} components have opposite signs. When we diagonalize the tensors we find the same eigenvalues and the same EFG for both sites. But due to differences in the local environments around the sites,the eigenvectors and therefore the directions of the EFG are not the same.

iii) Zr_2Cu forms in a simple tetragonal structure with lattice parameters given by a=3.22A° and c=11.18A°[25]. There are three atoms in the primitive cell, a Cu atom and two Zr atoms with same LDOS. To obtain the EFG we have performed calculation for a Cu site and a Zr site, using a cluster of 1338 atoms around these sites. In the Zr_2Cu structure, both the Zr and the Cu sites have axial symmetry around the c-axis and we have that the EFG tensor is diagonal at every site of the structure.

every site of the structure.

We find that the EFG at the Cu site is negative and along the c-axes. The p and d contributions are of the same order and have the same sign. The agreement between k-space and real space results is good within the expected margin of errors. The case of the Zr site is more interesting. We find that the angular asymmetry(11) for the p orbitals is very small in this case (of order of milielectrons), beyond the accuracy of our calculations. Because these differences are so small, even considering the factor of ten in the values of the radial integrals(see Table 2), the p and d contributions get to be of the same order. In both k-space and real space, our results show p and d contributions of opposite signs and a extremely small total EFG. The p and d contributions are small quantities with large errors and we cannot determine those differences within the accuracy of the calculations. All that we can say is that the EFG at the Zr site is very small, close to zero. The EFG at the Zr site in the Zr_2Cu has been inferred from TDPAC measurements[12] which use Hf as a probe. The experimental results give for this EFG a very small value (23 x 10^{13} esu . cm^{-3}) and the sign is unknown. It is interesting to note that measured values at the Zr sites in amorphous alloys of similar composition give values of EFG which are a factor of ten larger. It is easy to understand this fact in the light of our results. The angular asymmetries (11) for both p and d orbitals are usually of order of hundredths of electrons. Because the radial p integral is larger, the p contribution is normally dominant at the Zr site, usually a factor of ten larger than the d contribution.

small p contribution, which is of the same order of the d-term. In an amorphous environment such an accident will hardly happen. The p contribution will be dominant and an order of magnitude larger, giving rise to the observed values of the EFG.

V - CONCLUSIONS

We have performed real space and k-space LMTO-ASA calculations to find the EFG at all sites in three different crystalline Zr alloys: Zr_2Fe, Zr_3Fe and Zr_2Cu. We found that the EFG at the Fe site is positive in Zr_3Fe and negative in Zr_2Fe and obtained a extremely small value for the EFG at the Zr site in Zr_2Cu. In all cases, the calculated values were in good agreement with experimental results available in the literature. For the other calculated sites no experimental data was found. Our calculations for the EFG predict a positive sign for this quantity at the Zr site in Zr_2Fe and at the Zr1 site in Zr_3Fe, but a negative sign at the Zr2 site in Zr_3Fe. We also predict the direction of the EFG at all the sites.

It is interesting to note that the EFG at the Zr site in Zr_2Cu is an order of magnitude smaller than those of pure Zr and all other Zr sites considered here. We show that the small value observed for the EFG in Zr_2Cu is due to the unusually small value of the usually dominant p contribution in this structure. This anomaly is due to the local symmetry around the Zr site in crystalline Zr_2Cu and should not be present in the case of Zr sites in amorphous Zr-Cu alloys of similar composition. Therefore, as it

in amorphous Zr-Cu alloys of similar composition. Therefore, as it is to be expected from our results, measured values for the EFG at Zr sites in the amorphous alloys are one order of magnitude larger than those observed for the Zr site in Zr_2Cu.

In the case of Zr_2Cu we have axial symmetry and the value for the asymmetry parameter η is zero at both sites. In the case of Zr_2Fe, again due to axial symmetry, η is equal to zero at the Fe site, but we find an extremely large value of η (around 0.7) at the Zr site for this structure. In the case of Zr_3Fe there is no axial symmetry, but the measurements indicate that η is close to zero. We have used this information to obtain the position parameters of Fe in the structure. The parameter η at the Zr sites in Zr_3Fe were found to be finite, but very small.

In conclusion, we have shown that the real-space LMTO-ASA-TB scheme, when applied to obtain the EFG in close packed metallic binary alloys, is reliable and reproduces well results obtained by regular reciprocal space methods and experiment. We have also obtained detailed information about the EFG in the Zr compounds considered here.

Acknowledgments

We wish to thank Professor O.K. Andersen and his group and Dr. M.S. Methfessel for very useful discussions and for making available to us the programs used in the k-space part of this work. We also wish to thank Dr. H. Rechenberg for comments regarding the measured EFG.

This work was partially supported by Financiadora de Estudos e Projetos (FINEP) and Conselho Nacional de Desenvolvimento Cientifico e Tecnológico (CNPq).

Referências:

01- E.N. Kaufmann and R.J. Vianden, Rev. Mod. Phys. 51, 161(1979).

02- R. Vianden, Hyperfine Interact. 15/16, 189(1983).

03- T.P. Das and P.C. Schmidt, Z. Naturforsch. 41a, 47(1986).

04- G. Cjzek, J. Jink, F. Gotz, H. Schmidt, J.M.D. Coey, J.P. Reboillat and A. Lienard, Phys. Rev. B 23, 2513(1981).

05- D. Guenzburger and D.E. Ellis, Phys. Rev. B 36, 6971(1987).

06- P. Blaha, K. Schwarz and P.H. Dederichs, Phys. Rev. B 37, 2792(1988).

07- H.M. Petrilli and S. Frota-Pessôa, J. Phys. Condens. Matter 2, 135(1990).

08- O.K. Andersen and O. Jepsen, Phys. Rev. Lett. 53, 2571(1984).

09- M. Methfessel and S. Frota-Pessôa, J. Phys. Condes. Matter 2, 149(1990).

10- H.M. Petrilli, S. Frota-Pessôa and M. Methfessel, Hyp. Int. 60, 647(1990).

11- H.M. Petrilli and S. Frota-Pessôa, Hyp. Int. 60, 643(1990).

12- L.A. Mendoza - Zelis, L.C. Damonte, A.G. Bibiloni, J. Desimoni and A. Lopez-Garcia, Phys. Rev. B 34, 2982(1986).

13- A.L. Yeyati, M. Weissmann and A.L. Garcia, Phys. Rev. B 37, 10608(1988).

14- M. Maurer, J.M. Friedt and J.P. Sanchez, J. Phys. F: Met. Phys. 15, 1449(1985).

15- J.M. Friedt, M. Maurer, J.P. Sanchez, J. Vincze, A. Bonnenfant, C. Paliudis, M.M. ABD-Elmeguid and H. Micklitz, Rap. Quench. Met. 533(1985).

16- H.M. Petrilli and S. Frota-Pessôa, Solid State Commun. 77,103(1991).

17- R. Haydock, Solid State Phys. 35, 216(New York:Academic, 1980).

18- S. Ferreira. J. Duarte Jr. and S. Frota-Pessôa, Phys. Rev. B, 41, 5627(1990).

19- O. K. Andersen, O. Jepsen and D. Glötzel in "Highlights of Condensed Matter Theory, edited by F. Bassani, F. Fumi and M. P. Tosi (North-Holland, Amsterdan,1985)

20- O.K. Andersen, in "The Electronic Structure of Complex Systems", edited by P. Pharisean and W.M. Temmerman(Plenum, New York, 1983).

21- N. Beer and D. G. Pettifor, in "The Electronic Structure of Complex Systems, edited by W. Temmerman and P. Phariseau (Plenun, New York, 1984).

22- E. E. Havinga, H. Damsma and P. Hokkeling, J. Less-Common Met 27, 169 (1972).

23- I. Vincze, F. Van der Woude and M. G. Scott, Solid State Commun. 37, 567 (1981).

24- B. Aronsonn, M. Backman and S. Rundqvist, Acta Chem. Scand. 14, 1001 (1970).

25- M. V. Nevitt and J. W. Downey, AIME Trans. 224, 195 (1962).

		EFG(R)	EFG(k)	EXP
Zr_2Fe	Fe	- 66	- 96	- 134
	Zr	+ 269	+ 322	—
Zr_3Fe	Fe	+ 193	+ 243	+ 147
	Zr1	+ 231	+ 225	—
	Zr2	- 194	- 139	—
Zr_2Cu	Zr	≃ 0	≈ 0	± 23
	Cu	- 142	- 102	—

TABLE 1 - EFG in units of 10^{13} esu.cm^{-3} for Zr_2Fe, Zr_3Fe and Zr_2Cu obtained in real-space (R) and k-space (k) as compared with experimental results from ref(14) and ref (12).

	I_{pp} ($Å^{-3}$)	I_{dd} ($Å^{-3}$)
Zr (hcp)	95.68	12.22
Fe (bcc)	58.16	30.25
Cu (fcc)	48.90	53.03

TABLE 2 - Radial Integrals for the pure metals

$T(\vec{k})$	T(R)	$p(\vec{k})$	p(R)	$d(\vec{k})$	d(R)	Eigenvectors
-271	-239	-252	-220	-19	-19	-0.70;+0.71; 0.00
-51	-30	-47	-28	-4	-2	0.00; 0.00; 1.00
+322	+269	+299	+248	+23	+21	+0.71;-0.70; 0.00

Table 3 - EFG tensor (in units of 10^{13} esu.cm^{-3}) in the principal axes at the Zr site in Zr_2Fe. Eigenvalues (EFG tensor components) for the total(T), p and d contributions obtained from real-space(R) and k-space($\vec{k}$) calculations.

$T(\vec{k})$	Eigenvectors ($\vec{k}$)	T(R)	Eigenvectors (R)
-139	0.00; 0.51; 0.86	-194	0.00; 0.64; 0.77
+62	0.00;-0.86; 0.51	+50	0.00;-0.77; 0.64
+77	1.00; 0.00; 0.00	+144	1.00; 0.00; 0.00

TABLE 4 - EFG tensor (in units of 10^{13} esu.cm^{-3}) in the principal axes at the Zr2 site in Zr_3Fe. Eigenvalues (EFG tensor components) and corresponding eigenvectors obtained from real space(R) and k-space($\vec{k}$) calculations.

FIGURE CAPTIONS

FIGURE 1 - Positions of Zr atoms(large spheres) and Fe atoms (small spheres) in Zr_3Fe, projected in the plane perpendicular to the a-axes. The empty spheres are located in the plane x=0 and the dashed spheres are located in the plane x=(a/2). Arrows indicate the directions of the displacements of the Fe sites when the Fe position parameter y is varied.

FIGURE 2 - Components of the EFG tensor (in units of 10^{13} esu.cm^{-3}) at the Fe site in Zr_3Fe along the b-axes (V_{yy}) and c-axes (V_{zz}) as a function of the Fe position parameter.

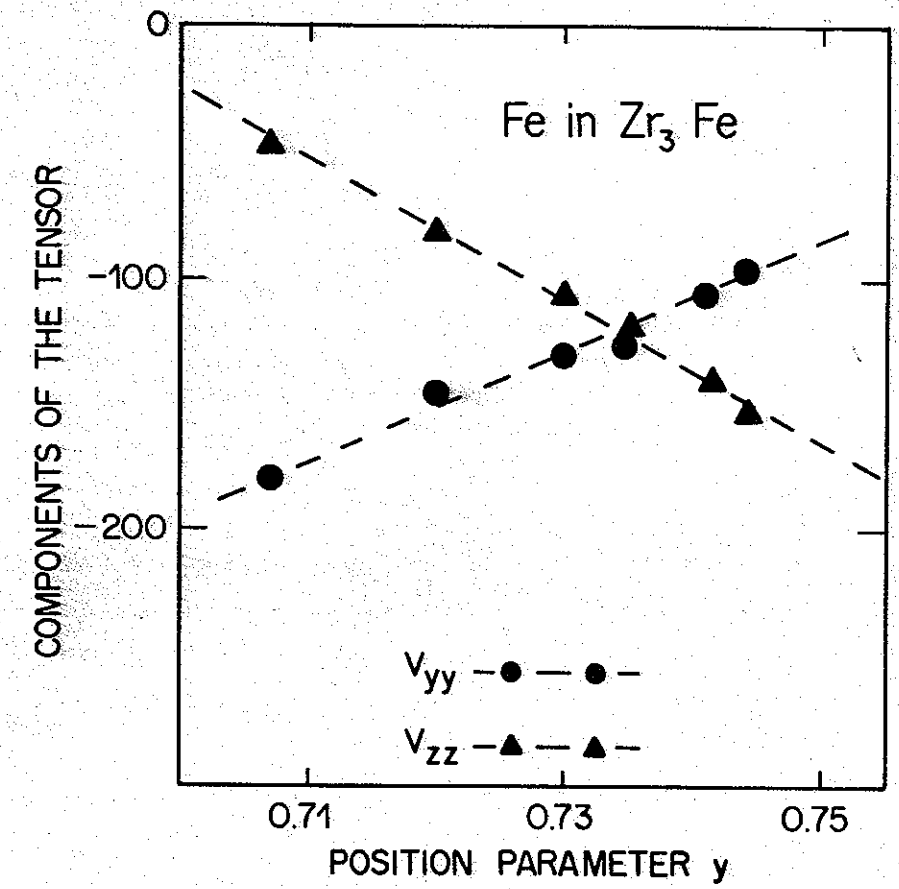
Fe in Zr_3 Fe
COMPONENTS OF THE TENSOR
0
-100
-200
V_{yy}
V_{zz}
0.71
0.73
0.75
POSITION PARAMETER y

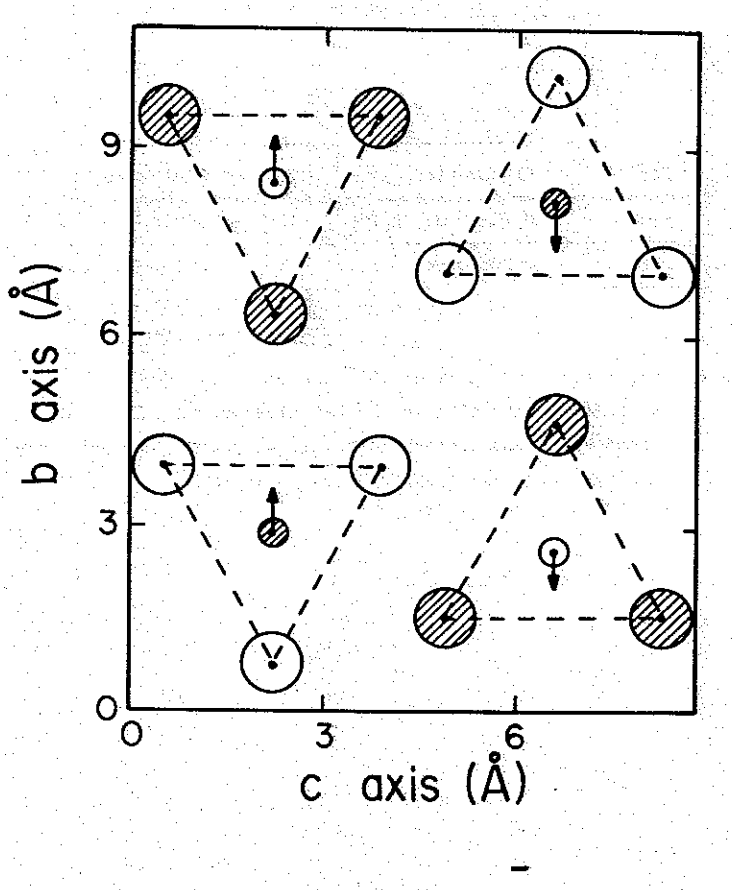
b axis (Å)
0
3
6
9
0
3
6
c axis (Å)